Original Research

Combined Helium-3/Proton Magnetic Resonance Imaging Measurement of Ventilated Lung Volumes in Smokers Compared to Never-Smokers

Neil Woodhouse, DCR,[1]* Jim M. Wild, PhD,[1] Martyn N.J. Paley, PhD,[1] Stanislao Fichele, PhD,[1] Zead Said,[1] Andrew J. Swift,[1] and Edwin J.R. van Beek, PhD, MD[1,2]

Purpose: To use a combination of helium-3 (3-He) magnetic resonance imaging (MRI) and proton single-shot fast spin echo (SSFSE) to compare ventilated lung volumes in groups of "healthy" smokers, smokers diagnosed with moderate chronic obstructive pulmonary disease (COPD), and never-smokers.

Materials and Methods: All study participants were assessed with spirometry prior to imaging. 3-He images were collected during an arrested breath hold, after inhaling a mixture of 200 mL of hyperpolarized 3-He/800 mL of N_2. Proton SSFSE images were acquired after inhaling 1 liter of room air. The ventilated volume for each study participant was calculated from the 3-He images, and a ratio was calculated to give a percentage ventilated lung volume.

Results: Never-smokers exhibited a 90% mean ventilated volume. The mean ventilated lung volumes for healthy smokers and smokers diagnosed with COPD were 75.2% and 67.6%, respectively. No correlation with spirometry was demonstrated for either of the smoking groups.

Conclusion: Combined 3-He/Proton SSFSE MRI of the lungs is a noninvasive method, using nonionizing radiation, which demonstrates ventilated airspaces and enables the calculation of ventilated lung volumes. This method appears to be sensitive to early obstructive changes in the lungs of smokers.

Key Words: hyperpolarized helium-3 MRI; lung volumes; smoking; image segmentation
J. Magn. Reson. Imaging 2005;21:365–369.
© 2005 Wiley-Liss, Inc.

HYPERPOLARIZED HELIUM-3 (3-He) magnetic resonance imaging (MRI) is an emerging technique, which has been shown to produce high-resolution images of ventilated human airspaces (1,2). Proton MRI of the lungs has long been regarded to be of limited use in lung imaging due to cardiac motion artifacts, low proton density, and large magnetic susceptibility gradients associated with lung tissue. However, with ongoing development of fast imaging sequences, proton MRI of the lungs is now enjoying somewhat of a renaissance (3,4). In this work single-shot fast spin echo (SSFSE) breath-hold images of the lungs were used to calculate a thoracic volume (5), and 3-He ventilation images were used to calculate a ventilated volume (6–8) for each study participant. A ratio of ventilated volume to thoracic volume was calculated to give a percentage ventilated lung volume.

MATERIALS AND METHODS

The local research ethics committee gave approval, and written informed consent was obtained from each study participant. The lungs of 13 volunteers (5 male, 8 female; mean age = 51; range = 40–62) and 5 patients with chronic obstructive pulmonary disease (COPD) (2 male, 3 female; mean age = 53; range = 47–61) were imaged using proton SSFSE MRI and 3-He MRI in the coronal plane. All participants were assessed with spirometry prior to imaging and assigned to three groups: eight healthy never-smokers, five "healthy" smokers with a smoking history of >10 pack years, and five smokers with moderate COPD as demonstrated by spirometry and clinical history. Thus, COPD was defined as a subject who is symptomatic (chronic cough and shortness of breath), and the spirometric indices are 30% < forced expiratory volume in one second (FEV1) < 80% of the predicted value in combination with an FEV1/forced vital capacity (FVC) < 70%. Reversibility of spirometric indices was less than 12% and less than 200 mL. Neither the never-smokers nor the healthy smokers exhibited obstructive spirometric indices. Both MRI examinations were performed on a 1.5-T whole-body system (Eclipse, Philips Medical Systems, Cleveland, OH, USA), which was modified to transmit and receive at the 3-He frequency of 48 MHz. 3-He images were acquired with a flexible quadrature trans-

[1]Unit Academic of Radiology, University of Sheffield, Royal Hallamshire Hospital, Sheffield, UK.
[2]Carver College of Medicine, University of Iowa Hospitals and Clinics, Department of Radiology, Iowa City, Iowa, USA.
This work was presented at the 11th Annual Meeting of ISMRM, Toronto, 2003 (Poster 1399).
*Address reprint requests to: N.W., Unit of Academic Radiology, Floor C, Royal Hallamshire Hospital, Glossop Road, Sheffield, S10 2JF, United Kingdom. E-mail: n.woodhouse@sheffield.ac.uk
Received May 18, 2004; Accepted December 17, 2004.
DOI 10.1002/jmri.20290
Published online in Wiley InterScience (www.interscience.wiley.com).

© 2005 Wiley-Liss, Inc.

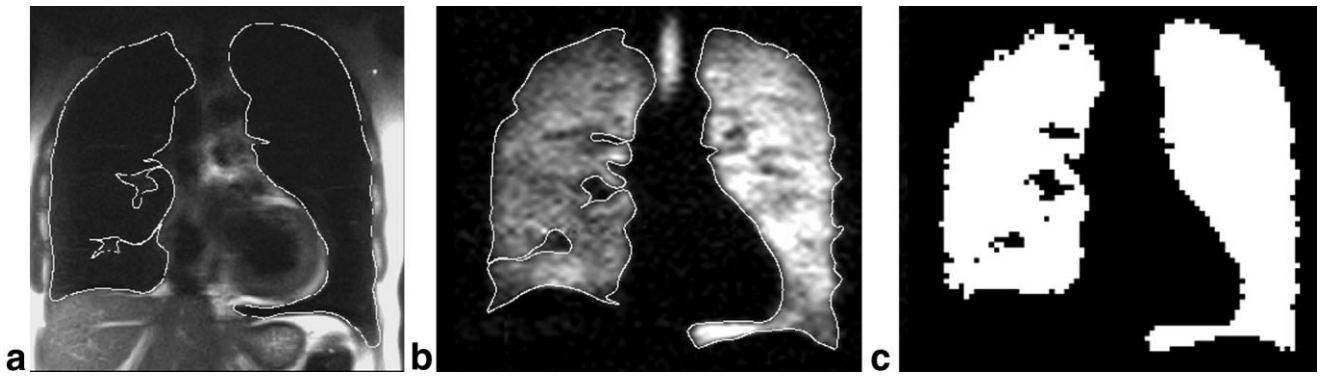

Figure 1. Manually and automatically defined regions of interest in a never-smoker. **a:** Manually defined region of interest for thoracic volume in SSFSE image, the mediastinum, and large pulmonary vessels were excluded from the region of interest. **b:** Manually defined region of interest for 3-He ventilation image with homogenous distribution of 3-He through the lungs. **c:** Binarized 3-He ventilation image. Ventilated volume was calculated from the voxel count.

mit/receive coil. 3-He gas was polarized on site to approximately 30% using a spin exchange polarizer (GE Healthcare, Princeton, NJ, USA). For the 3-He ventilation study, 19 contiguous slices were collected during a 14-second arrested inspiration after inhaling a mixture of 200 mL of 3-He /800 mL of N_2 from a Tedlar® bag (Jensen inert products, Coral Springs, FL, USA) from a starting point of functional residual capacity (FRC). The imaging sequence was a two-dimensional gradient recalled echo (TR = 131 msec, TE = 3.4 msec, flip angle = 9°, field of view (FOV) = 400 mm, slice thickness = 12 mm, matrix = 112 views × 128 samples, 1 NEX). Phase encoding order was centric to maximize signal-to-noise ratio (SNR) (9). The proton MR images were acquired during 20 seconds of arrested inspiration after inhaling 1 liter of room air from an identical Tedlar® bag (reproducing the breath-hold procedure of the 3-He scan). The sequence used was an SSFSE (TE effective = 61.1 msec, echo train length (ETL) = 140, flip angle = 90°, FOV = 400 mm, slice thickness = 10 mm, matrix = 256 × 256, 1 NEX). The proton images were acquired using a flexible receive-only phased array coil. The ventilated lung volume for each volunteer was calculated from the 3-He images by manual segmentation of signal intensity (Fig. 1b). Thoracic volumes were calculated from the proton SSFSE scans by manual segmentation of the signal void (5) (Fig. 1a). The anatomic dead space, i.e., the trachea and main bronchi, was not included in the regions of interest (ROI) for either study. Two observers blinded to patient clinical details executed the image segmentation. A ratio of ventilated volume/thoracic volume was calculated to give a percentage ventilated lung volume for each subject. The mean percentage ventilated lung volume for each subject group was then calculated with a 95% confidence interval (95% C.I.). Interobserver error was assessed on a slice-by-slice basis using the Pearson correlation coefficient. The interobserver error was further analyzed at the hilar regions of the lungs on both sets of images. The 3-He images were also segmented semiautomatically using in-house developed Matlab® code to binarize the images (Fig. 1c) using a threshold value derived from the SNR of each image.

$$\text{Threshold} = \text{Mean Signal} - (3*\text{S.D. Noise})$$

The noise was sampled from a 10*10 pixel area at the edge of the image, and the signal was sampled from an interactive user-defined ROI within the lungs. A signal-dependent thresholding method was chosen rather than a fixed threshold (6,8), as the SNR of the images varied throughout the data set for each subject. All pixel values below the threshold were assigned a value of zero, and all pixel values above the threshold were assigned a value of one, the ones were counted to give

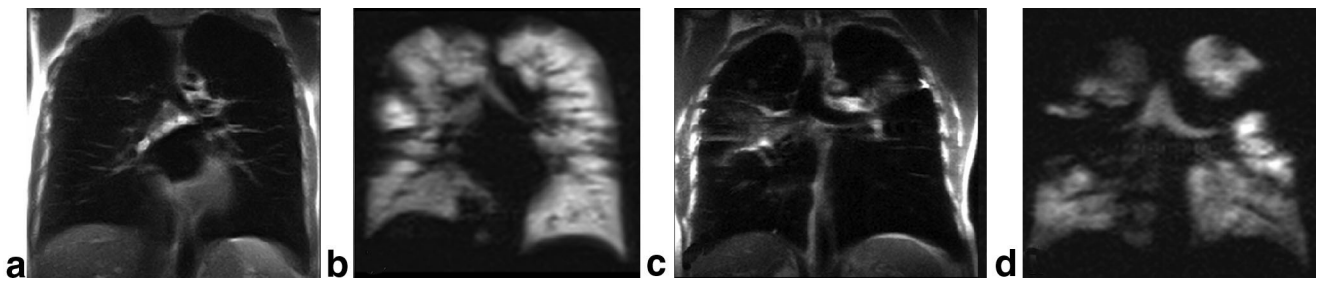

Figure 2. Proton SSFSE and 3-He ventilation in smokers. **a:** Proton SSFSE breath-hold image from a "healthy smoker." **b:** Corresponding 3-He image to (a) showing ventilation defects in the lungs of a "healthy" smoker with no obstructive defect demonstrated by spirometry. **c:** Proton SSFSE image from a smoker diagnosed with COPD showing hilar lung disease. **d:** Corresponding 3-He image to (c) demonstrating large ventilation defects and inhomogeneous distribution of 3-He.

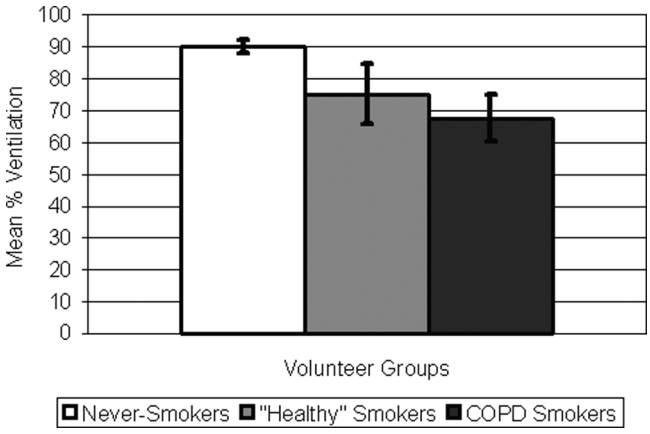

Figure 3. Mean percentage ventilated lung volumes for each of the three volunteer groups are displayed together with the 95% confidence interval.

an area for each slice. The manually segmented ROIs were compared slice-by-slice to the thresholded areas for interobserver error using the Pearson correlation coefficient. The ventilated volumes were also compared to the percent predicted FEV_1/FVC spirometric index, which is a measure of airway obstruction, using the Pearson correlation coefficient and least squares regression analysis. All images were also assessed for quality and ventilation distribution by a consultant radiologist.

RESULTS

The never-smoking group demonstrated mainly homogeneous distributions of 3-He throughout the lungs (Fig. 1); ventilation defects if present were all reported as minor and mainly located at the periphery of the lung. The difference in volume between the proton SSFSE and the 3-He scans for the never-smoking group gave a 90%, 95% C.I. (87.87, 92.13) mean ventilated volume. All subjects in both groups of smokers exhibited ventilation defects on the 3-He ventilation images (Fig. 2), the majority of these defects being classified by a radiologist as either medium or large. The healthy asymptomatic group of smokers was found to have a mean ventilated volume of 75.2%, 95% C.I. (65.73, 84.67). The group of smokers with diagnosed COPD demonstrated the lowest mean ventilated lung volume of 67.6%, 95% C.I. (60.17, 75.03). These results are presented in Fig. 3. Interobserver correlation was high in both sets of images for all patient groups (Table 1). The main source of disagreement between observers occurred in the hilar regions of the lungs in all groups; the hilar region was defined as the central five slices of each data set, with the middle slice centered on the bifurcation of the trachea. This interobserver disagreement is reflected in the lower correlation coefficients observed when ROIs in the hilar regions were assessed separately (Table 2). The semiautomated thresholding method of segmentation produced good results, removing background noise and preserving signal in the lung fields (Fig. 1c). The manually segmented ventilation images were compared to the semiautomatically segmented images on a slice-by-slice basis to assess observer bias. The Pearson correlation coefficients for observers 1 and 2 were 0.95 and 0.94, respectively ($P < 0.05$). Regression analysis of the manually segmented images and the automatically segmented images produced a good fit for both observers (Fig. 4). When the percentage ventilated volumes of the entire group were compared to the FEV_1/FVC results obtained at spirometry, a correlation coefficient of 0.72 was demonstrated and regression analysis produced a slight trend with an R^2 value of 0.515 (Fig. 5). However, when the groups were assessed individually, only a slight correlation was observed in the nonsmoking group (0.58), and no correlation or trend was demonstrated in either the healthy smokers or the COPD group, where correlation coefficients of 0.28 were observed in both groups.

DISCUSSION

Lung volumes were measured using proton SSFSE and 3-He MRI techniques, and the resultant percentage ventilated lung volume was shown to be significantly different between a population of never-smokers and a group of smokers with or without smoking-related COPD. All groups (including the never-smoking control group) exhibited a mean negative difference in lung volume. The 90% ventilated volume in the never-smokers could be attributable to a combination of minor ventilation defects in some subjects and loss of signal in the 3-He images through magnetic susceptibility field gradients at the lung periphery (10). Similarly, susceptibility field gradients may also contribute to artifacts or signal reductions in the proton scans, leading to an overestimation the thoracic volume. This signal loss through susceptibility effects would also be expected to apply equally to both groups of smokers. The COPD group exhibited the lowest ventilated volume, followed by the "healthy" smokers. The overlap of the confidence indices between the two groups of smokers in Fig. 3, coupled with the fact that the FEV_1/FVC did not correlate with the percentage ventilated volume in either group of smokers, may indicate that the severity of lung disease in some of these apparently healthy smokers is greater than indicated by spirometry. However, the noncorrelation of spirometric indices with the ventilated volumes observed in the individual groups could also be due to the small sample sizes present. The

Table 1
Interobserver Correlation for Manual Segmentation

	Never-smokers	Healthy smokers	COPD smokers	All groups together
Proton SSFSE volume	0.98	0.99	0.97	0.98
Helium-3 volume	0.99	0.98	0.98	0.98

Table 2
Interobserver Correlation at the Hilar Regions

	Never-smokers	Healthy smokers	COPD smokers	All groups together
Proton hilar region	0.82	0.96	0.77	0.85
Helium hilar region	0.87	0.82	0.98	0.89
Overall correlation	0.85	0.89	0.87	0.87

interobserver correlation was high in all groups, although slightly lower in the proton scans for the COPD group, which led us to investigate where the greatest area of disagreement was. The Pearson correlation coefficient for the hilar region of the SSFSE scans (Table 2) was much lower for the COPD group, and this may be attributable to this group being less able to hold their breath for the required period, introducing some movement artifact into the images. Also, the presence of some hilar lung disease (Fig. 2c) in this group of patients meant that more complex ROIs had to be defined, which could also have contributed to a higher level of disagreement between observers. Automated ROI definition by signal intensity thresholding is simple enough to implement in the case of the 3-He ventilation images, as helium signal is either present or not, and no other structures apart from the lungs, trachea, and bronchi are demonstrated. However, when segmenting the thoracic cavity from the proton SSFSE images, many other structures have similar signal characteristics to the lung fields, e.g., the signal void from flowing blood in major blood vessels, and defining a threshold value becomes more problematic. After considering these apparent drawbacks and comparing this sequence with bright-blood sequences such as steady-state free precession (SSFP) and fast low angle shot (FLASH) (with gradient motion rephasing), it was decided that the lack of cardiac motion artifacts on the SSFSE sequence made segmentation easier, and that electrocardiogram (ECG) triggering of the bright-blood sequences would have made the breath-hold period too long. We felt that it was important to use the same method of segmentation (manual) for both sets of images, to be able to compare the results objectively, and the semiautomated thresholding method was used to rule out observer bias only. An advantage of the manual approach is that only the manufacturers' software is required to perform the image analysis, enabling simple and reproducible implementation of this method on any MRI system capable of 3-He imaging. Another source of error could arise from the changing of coils in between 3-He and proton SSFSE examinations; however, the coils were of exactly the same dimensions, so although the subjects were repositioned in between examinations, the scanning position was reproducible. This was not an attempt to measure absolute lung volumes with MRI. Studies that have correlated MRI volumetry with physiological measures such as spirometry have used airspace:tissue ratios (6) or other correction formulae to account for the differences in lung volumes in the sitting and supine positions (7). Correction factors were not necessary in this study, as both methods used are equally insensitive to parenchymal volume, and both examinations were performed in the supine position. Both breath-hold maneuvers were as near identical as possible due to the fixed volume of gas inhaled from the bag and same starting position, enabling direct comparison. As a result, however, the volumes measured are not comparable to a physiological value such as total lung capacity, since it is unlikely that the majority of the subjects' lungs would have been fully inflated following the inhalation of 1 liter of gas from a starting point of FRC. In conclusion, combined 3-He/proton SSFSE MRI of the lungs is a noninvasive method, using nonionizing radiation, which demonstrates the distribution of gas in the ventilated airspaces, and enables the calculation of ventilated lung volumes. This method appears to be sensitive to early obstructive changes in

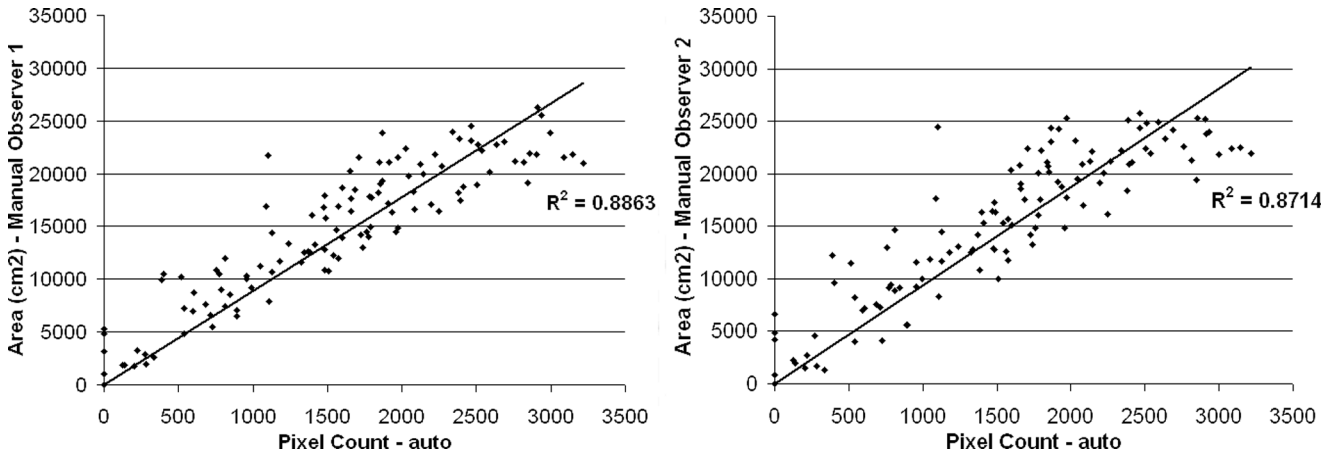

Figure 4. Slice by slice regression analysis of manually segmented regions of interest vs. semiautomatic pixel counting gave good fits for both observers.

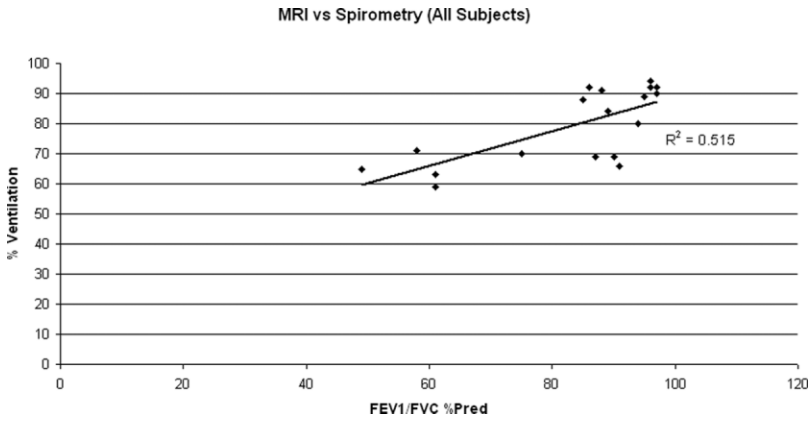

Figure 5. Least squares regression analysis of ventilated volume vs. FEV_1/FVC for all subjects revealed only a slight trend. This was not regressed through zero as the two techniques are not directly comparable due to total lung capacity not being reached for the MRI examination, and the different postures for each; (supine for MRI and sitting for spirometry).

the lungs and may be a useful tool supplementary to spirometry in the diagnosis and follow-up of obstructive lung disease. The manual segmentation method gives easily reproducible results in normal and diseased lungs for both 3-He ventilation and SSFSE images. Manual segmentation of 3-He ventilation images correlates well with semiautomatic thresholding of the same images. This method of assessing ventilated lung volumes may provide a more objective method of scoring 3-He MRI scans than a subjective estimation of the severity of ventilation defects (11).

ACKNOWLEDGMENTS

We are grateful for the loan of commercial helium-3 gas polarizer from GE-Health (Princeton, NJ) and technical support from Spectra Gases (Huntingdon, UK) and Philips Medical Systems (Best, The Netherlands).

REFERENCES

1. Moller HE, Chen XJ, Saam B, et al. MRI of the lungs using hyperpolarized noble gases. Magn Reson Med 2002;47:1029–1051.
2. Kauczor HU, Hanke A, van Beek EJ. Assessment of lung ventilation by MR imaging: current status and future perspectives. Eur Radiol 2002;12:1962–1970.
3. Kauczor HU, Kreitner, KF. MRI of the pulmonary parenchyma. Eur Radiol 1999;9:1755–1764.
4. Hatabu H, Gaa J, Eiji T, Edinburgh KJ, Stock EG, Edelman RR. MR imaging of pulmonary parenchyma with a half-Fourier single-shot turbo spin-echo (HASTE) sequence. Eur J Radiol 1999;29:152–150.
5. Qanadli SD, Orvoen-Frija E, Lacombe P, DiPaola R, Bittoun J, Frija, G. Estimation of gas and tissue lung volumes by MRI: functional approach of lung imaging. J Comput Assist Tomogr 1999;23:743–748.
6. Kauczor HU, Markstaller K, Puderbach M, et al. Volumetry of ventilated airspaces by 3He MRI: preliminary results. Invest Radiol 2001;36:110–114.
7. Markstaller K, Kauczor HU, Puderbach M, et al. 3He-MRI-based vs. conventional determination of lung volumes in patients after unilateral lung transplantation: a new approach to regional spirometry. Acta Anaesthesiol Scand 2002;46:845–852.
8. Zaporozhan J, Ley S, Gast KK, et al. Functional analysis in single-lung transplant recipients: a comparative study of high-resolution CT, 3He-MRI, and pulmonary function tests. Chest 2004;125:173–181.
9. Wild JM, Paley MN, Viallon M, Schreiber WG, van Beek EJ, Griffiths PD. k-space filtering in 2D gradient-echo breath-hold hyperpolarized 3He MRI: spatial resolution and signal-to-noise ratio considerations. Magn Reson Med 2002;47:687–695.
10. Wild JM, Fichele S, Woodhouse N, et al. Assessment and compensation of susceptibility artifacts in gradient echo MRI of hyperpolarized 3He gas. Magn Reson Med 2003;50:417–422.
11. Donnelly LF, MacFall JR, McAdams, et al. Cystic fibrosis: combined hyperpolarized 3He-enhanced and conventional proton MR imaging in the lung—preliminary observations. Radiology 1999;212:885–889.